Available online at www.CivileJournal.org

Civil Engineering Journal

(E-ISSN: 2476-3055; ISSN: 2676-6957)

Vol. 10, Special Issue, 2024
"Sustainable Infrastructure and Structural Engineering:
Innovations in Construction and Design"

Artificial Intelligence Models for Predicting the Compressive Strength of Geopolymer Cements

Cut Rahmawati [1, 2*], Siti Aisyah [3], Sanusi [4], Iqbal [5], M. Mufid Maulana [1], Erdiwansyah [6], Jawad Ahmad [7]

[1] *Department of Civil Engineering, Engineering Faculty, Universitas Abulyatama, Aceh Besar, 23372, Indonesia.*

[2] *Advanced Materials and Nanotechnology Research Center (MatNano), Universitas Abulyatama, Aceh Besar, 23372, Indonesia.*

[3] *Faculty of Technology and Computer Science, Universitas Prima Indonesia, Indonesia.*

[4] *Department of Information Technology, Engineering Faculty, Universitas Teuku Umar, Aceh Barat, 23615, Indonesia.*

[5] *Department of Mechanical Engineering, Engineering Faculty, Universitas Abulyatama, Aceh Besar, 23372, Indonesia.*

[6] *Faculty of Engineering, Universitas Serambi Mekkah, Banda Aceh 23245, Indonesia.*

[7] *Department of Civil Engineering, Military College of Engineering, NUST, Risalpur, 24080, Pakistan.*

Received 16 October 2023; Revised 11 April 2024; Accepted 03 May 2024; Published 26 May 2024

Abstract

The utilization of nanosilica and cellulose nanocrystals (CNCs) in cement geopolymers remains challenged by intricacies and uncertainties regarding their concentration, posing difficulties in the formulation of systematic geopolymer mix designs. This study aims to formulate models based on Artificial Neural Networks (ANN) capable of forecasting the compressive strength of geopolymers through the utilization of experimentally acquired data. Nanosilica was applied at concentrations of 2%–4% and CNCs at 1%–3%. ANN was modeled using MATLAB to predict the compressive strength of the geopolymer. The results indicated an effect of nanosilica and CNCs on the compressive strength of geopolymer at 2%–4% concentration and 1%–3% CNCs. The best ANN was the GDX training function, purelin activation function, LGD and LGDM learning functions, Lr 0.1 and 0.01 at the number of epochs 3812 out of 25000 and 1774 out of 25000, resulting in the best correlation values of 0.994 and 0.959; the lowest RMSE values are 0.022 and 0.110. The results of the ANN model built based on actual data prove that the model is helpful for accurate simulation to predict the compressive strength of geopolymer cement. This study contributes novelty by optimizing the design model for Geopolymer Cements incorporating nanosilica and CNCs.

Keywords: Artificial Neural Network; Nanosilica; Cellulose Nanocrystals (CNCs); A.Donax L.

1. Introduction

Geopolymers are inorganic aluminosilicate polymers produced by adding various aluminosilicates (waste rich in silicon and aluminum) and alkaline solutions as activators. The most common alkaline solution used in polymerization is a combination of sodium hydroxide (NaOH) and sodium silicate (Na_2SiO_3). Geopolymers have been composited with

* Corresponding author: cutrahmawati@abulyatama.ac.id

http://dx.doi.org/10.28991/CEJ-SP2024-010-03

different materials due to their excellent material properties and easy bonding with different materials. The use of geopolymer composites has attracted many researchers, such as the use of rice husk ash [1], glass waste [2], coconut fiber (coir) [3, 4], palm oil fuel ash (POFA) [5], and many more.

Nanotechnology plays a significant role in developing geopolymer composites, and nanomaterials have been designed to increase the mechanical strength of geopolymers [6–9]. Nanomaterials often added to geopolymers are nanosilica, but in its development, fiber has become the best alternative for improving the tensile strength of geopolymers. Fibers used in geopolymers must first be treated to remove unnecessary fiber parts that negatively affect the geopolymer. Cellulose nanocrystals (CNCs) are promising alternative materials in geopolymers. The CNCs that have been added to the geopolymers are sawdust [10], typha plants [11, 12], wood pulp [13], and CNCs provided by Sigma Aldrich Company [14].

Plant-derived fibers can reinforce cement-based products [15–19]. The fibers used in this study are from Arundo Donax L. This plant is a non-timber plant growing abundantly and naturally in Indonesia. Due to its high growth rate, it is an invasive and aggressive species, and its removal is complex. A. Donax L has a high cellulose content and can be applied to various needs [20]. The high growth rate of this plant allows access to significant raw material reserves. A. Donax L fiber has a tensile strength of 248 MPa with a Young's modulus of 9.4 GPa. This fiber can be modified into CNCs and composited with nanosilica to obtain the best compressive strength.

In this study, nanosilica was derived from Rice Husk Ash (RHA) due to the high silica content (91.78%) [21, 22]. Incorporating nanosilica exhibits good pozzolanic reactivity, and its capacity to fill pores plays a pivotal role in developing high-performance geopolymer cement [23]. The synergy between fly ash, nanosilica from rice husk ash, and cellulose nanocrystals (CNCs) derived from A. Donax L fibers will yield a geopolymer cement with exceptional performance characteristics.

The utilization of geopolymer cement in the construction industry is confronted with the challenge of discovering the appropriate, rapid, and accurate formulation to enable swift application. Previous studies have incorporated nanosilica in geopolymer mixtures ranging from 2% to 10% [24, 25] and CNCs at levels of 1% to 3% [26-28]. However, these studies have not yet been able to accurately predict the strength of geopolymers or find correlations between variables. Therefore, this study adopts an approach to predict the mechanical strength of the composite of these two materials. In recent years, machine learning techniques have been used by researchers to predict the properties of geopolymer materials. Artificial Neural Networks (ANN) have increased in popularity. It has accurately predicted geopolymers' strength properties in civil engineering applications and has been recently evaluated in many works [29–33]. So far, studies on predicting the compressive strength of nanosilica-based geopolymers and CNCs with artificial intelligence models are unfrequent.

The compressive strength of geopolymer paste with the addition of nanosilica and CNCs can be predicted by traditional mathematical statistical forecasting and by machine learning techniques. Currently, more attention is paid to the second, such as ANN, because traditional mathematics statistical forecasting methods use a lot of data. ANN studies complex systems and has been widely applied to predict the mechanical strength of geopolymers. The network can discover the correlation between variables from the example through iteration without requiring prior knowledge about the relationship between the investigated variables [29]. ANN tries each sample alternately, using the input to calculate answers compared with the experimental response obtained. If false, the ANN corrects the network by changing the internal connections. The trial-and-error processes continue until the network outputs match the pattern to a specified level of accuracy [30].

Accurate ANN based models on geopolymer concrete to predict flexural strength have been carried out and produce high prediction accuracy with R values in the range of 0.95 to 0.99 [34]. The ANN models also developed on geopolymers using class-F fly ash proved to be an efficient tool for predicting compressive strength with a value of 0.85 [35]. ANN models were also applied to geopolymer-based soil stabilization, showing that ANN could predict the compressive strength of stabilized soils [36]. The slump and strength of fly ash-based geopolymer can also be evaluated with ANN models where the results show The R-value of 0.91. ANN models are the most cost-effective and time-effective way to solve complex problems, especially in materials engineering [37]. Based on the literature review, it becomes evident that there is a lack of comprehensive studies elucidating the accurate compressive strength of nanosilica composites and CNCs within geopolymers. Therefore, it is imperative to undertake predictive analyses of geopolymer compressive strength using experimentally derived data.

Developing Artificial Intelligence Models for Predicting the Compressive Strength of Geopolymer Cements involved several stages. Firstly, a thorough review of the advancements in Artificial Neural Network (ANN) models in the context of geopolymer was conducted. Subsequently, the materials and methodology were delineated, encompassing the testing of ANN models alongside the employed prediction evaluation methods. Subsequently, we will present our findings to showcase the developed models' effectiveness and accuracy in predicting compressive strength. We will then discuss the results comprehensively, analyzing the implications and potential applications of our findings in the field of construction materials.

2. Materials and Methods

2.1. Material

The raw materials used were fly ash with an average particle size of 30 µm and white-coloured RHA from a rice refinery. The stem fiber of *A. Donax* L.. was collected in an open field. Figure 1 shows the *A. Donax L*. plant fiber and its TEM image. The chemical reagents used were NaOH (Merck®, 97%), Na_2SiO_3, H_2O_2 (Merck®, 50%), H_2SO_4 (Merck®, 95-98%). All chemicals were used without any further purification processes.

2.2. Synthesis Nanosilica and CNCs

Nanosilica was synthesized based on previous research [22] with a ball mill at 600 rpm for 10 hours, and the average particle size obtained was 339.09 nm. Synthesis of CNCs was conducted using *A. Donax L.* fibers, followed by acid hydrolysis process. The extraction and isolation method was carried out according to the method that has been done before [6]. From this process, CNCs with an average diameter of 50-95 nm are obtained and calculated using imageJ software. Figure 1 shows TEM Image from raw material.

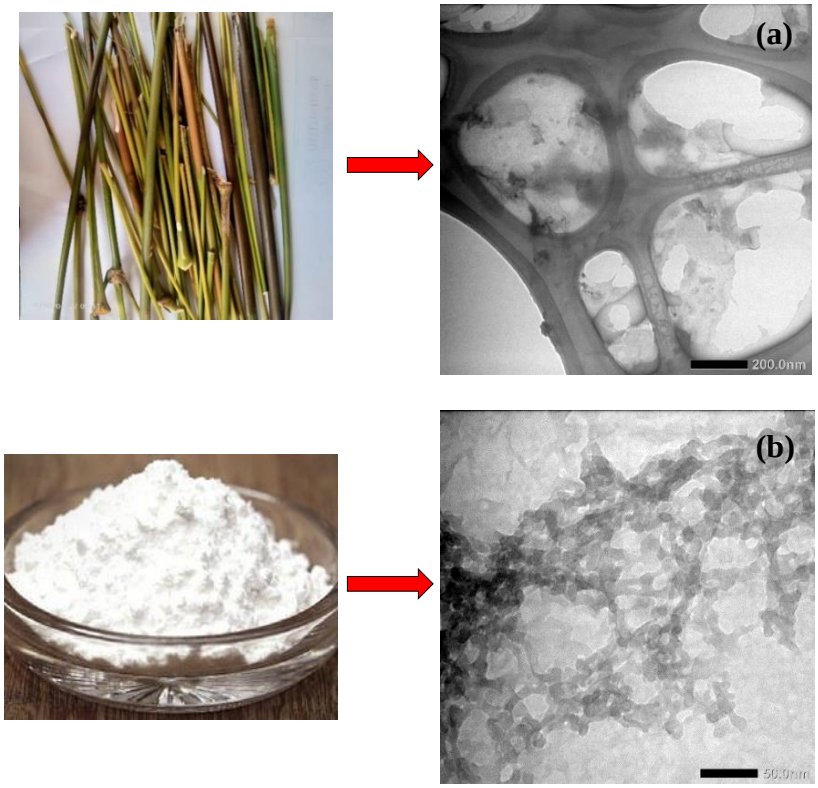

Figure 1. TEM Image from raw material (a) CNCs from A. Donax L fiber, (b) nanosilica from RHA

2.3. Process of Preparing Geopolymer Composites

The geopolymer paste was derived by mixing fly ash, nanosilica, and CNCs evenly and then adding the alkaline solution. The nanosilica concentration was 2%-4% while the CNCs were 1%-3%. This solution was prepared by dissolving 10 M NaOH with Na_2SiO_3 in a 1:1 ratio. The polymerization process hardened the geopolymer paste, and at the age of 28 days, compressive strength was tested.

2.4. Testing of ANN Model

This research used MATLAB application with ANN method by applying a backpropagation algorithm to predict compressive strength (MPa). The input data consisted of Nanosilica (%) and Cellulose Nanocrystals (%), while the compressive strength (MPa) was the target. Each input and target data variable amounted to 136 data. This study employs the multilayer backpropagation ANN algorithm. Backpropagation ANN is a feedforward neural network with multiple hidden layers and has been the preferred choice of researchers for data modeling. Figure 2 shows the modeling stages using the multilayer backpropagation ANN algorithm for model development.

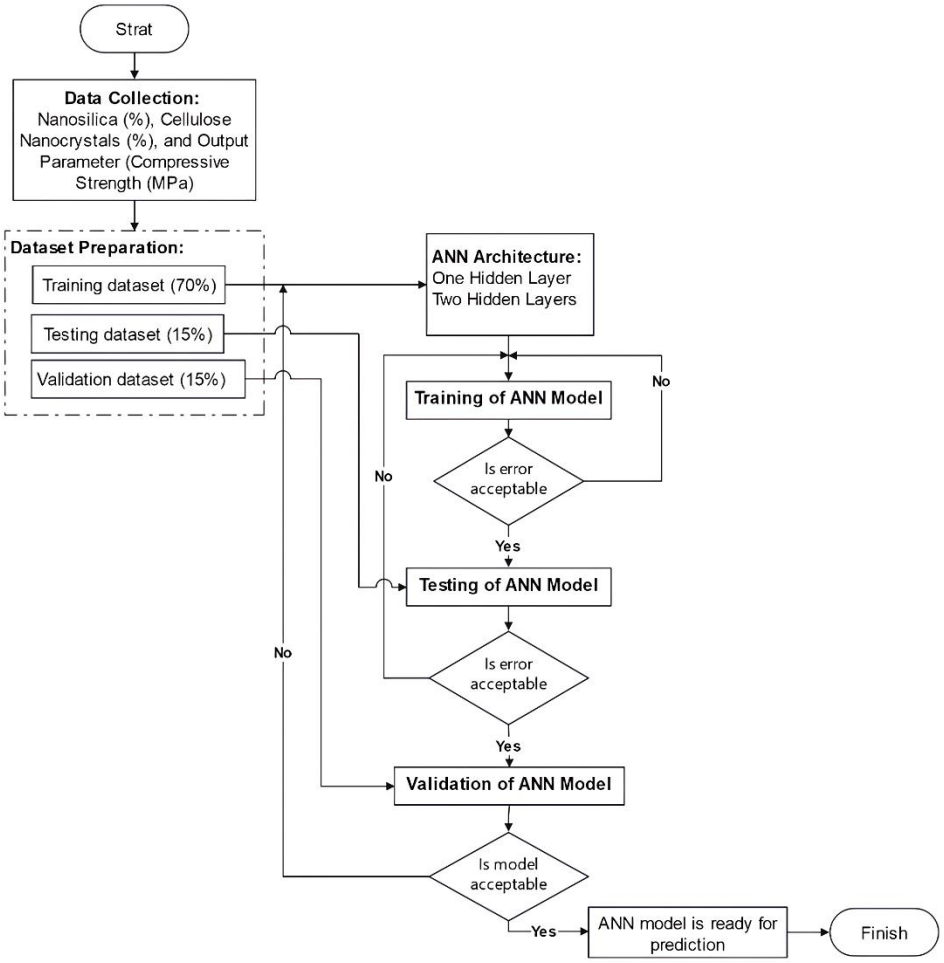

Figure 2. Flowchart of ANN Algorithm for Model Development

2.5. Artificial Neural Network Backpropagation (ANN-B) Modeling

Artificial Neural Network Backpropagation (ANN-B) is a statistical and non-statistical data modelling tool. ANN-B can perform complex correlation modelling between input and output to find patterns in the data. In general, the architecture of ANN-B consists of an input layer, a hidden layer, and an output layer. Furthermore, other parameters such as weight, bias, learning rate, threshold, and epoch are needed, which are already equipped in the MATLAB application. The activation functions used during the training and testing of the ANN-B model in this study are LOGSIG and PURLINE. The purelin activation function, or transfer function, is responsible for the connection between the input and output of a node in a neural network. The purelin or linear activation function is mathematically expressed as follows [38]:

$$f(x) = x \tag{1}$$

where $f(x) = x$ represents the identity function or linear function, this implies that the output of this function is equal to the input x provided.

2.6. Architecture of ANN-B

The ANN model's training, testing, and validation are divided into two stages. The first stage used random data with the ANN-B architecture consisting of one input layer, one hidden layer with 10, 20, and 30 neurons, and one output layer. This stage also used the training functions: Train-CGB, Train-GD, and Train-GDX. Each training function can be described as follows: Train-CGB is Conjugate gradient backpropagation with Powell-Beale restarts, Train-DG is Gradient descent backpropagation, and Train-GDX is Gradient descent with momentum and adaptive learning rate backpropagation. The PURLINE activation function or linear function was used in the output layer, which has the same output value as the input value, while the learning functions were LearnGD and LearnGDM. In general, the first ANN-B architecture is shown in Figure 3.

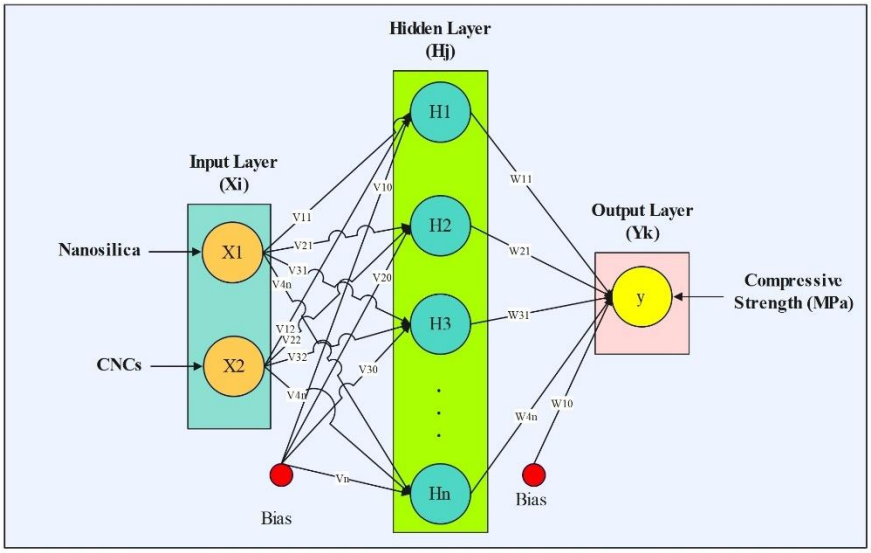

Figure 3. ANN-B Architecture with One Hidden Layer

The second stage of training, testing, and validation in the ANN model ANN-B architecture involves one input layer with two parameters: namely nanosilica and CNCs, two hidden layers comprising 10-30 neurons, and one output layer representing the prediction results. This stage differs slightly from the first stage, particularly in the configuration of the hidden layers. In the second stage, the hidden layers one and two consist of neurons as follows: 10; 10, 10; 20, and 20; 30 in the LearnGDM learning function (Gradient descent with momentum weight and bias learning function). The architecture of the second stage of ANN-B is illustrated in Figure 4.

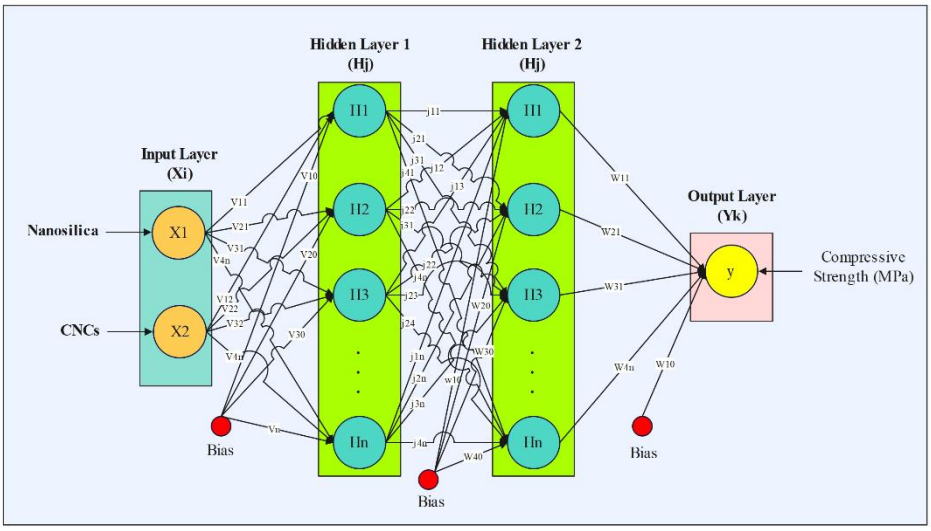

Figure 4. ANN-B Architecture with Two Hidden Layers

The algorithm used to obtain the modelling of the predicted compressive strength (MPa) with Nanosilica (%) and Cellulose Nanocrystals (%) as input data can be described in the simulation of Artificial Neural Network Backpropagation (ANN-B) as follows:

1. Prepare the Nanosilica vector data (%), Cellulose Nanocrystals (%) or (x1-x2), and the output compressive strength (MPa) or (Y), and determine the values of the weight, bias, learning rate, learning threshold, epoch, and activation function.
2. For each input unit to the hidden layer, z_j sums the weight of the input signal:

$$z\_in_j = b1_j + \sum_{i=1}^{n} x_i v_{ij} \quad (2)$$

Use the activation function to calculate the output signal $z_j = f(z\_in_j)$ and then send the signal to all units in its upper layer (output layer). Utilize the activation function to compute the output signal $z_j = f(z\_in_j)$ and subsequently transmit it to all units in its upper layer (output layer), z_in_j represents the initial process from the input layer to the

hidden layer, where $b1_j$ denotes the bias generated after the process from the input layer to the hidden layer to ascertain the error during the learning process. x_i denotes the input value, while v_{ij} signifies the weights in the hidden layer multiplied by each input value.

3. Each output unit (Y_k, k=1, 2, ..., m) is obtained by summing up the weighted of the input signals:

$$y\_in_k = b2_k + \sum_{i-1}^{p} z_i w_{jk} \quad (3)$$

Then use the activation function to calculate the output signal: $y_k = f(y\_in_k)$ and send those signals to all the units in the upper layer (output layer). y_{in_k}represents the output generated from the process of the hidden layer to the output layer, where $b2_k$ denotes the bias from the hidden layer to the output layer to determine the error during the learning process after passing through the process from the hidden layer to the output layer. z_i represents the value obtained in step 3, while w_{jk} signifies the weights in the hidden layer multiplied by each input value, thereby resulting in an output.

4. Each output unit (Y_k) receives a target pattern associated with the learning input pattern, and then the error information is calculated:

$$\delta_k=(t_k-y_k)\ f'(y\_in_k) \quad (4)$$

Then measure the weight correction (which will later be used to correct the w_{jk} value):

$$\Delta w_{jk} = \delta\alpha_k z_j \quad (5)$$

$$\Delta b2_k = \delta\alpha_k \quad (6)$$

$$w_{jk}(new)=w_{jk}(past) + \Delta w_{jk} \quad (7)$$

$$b2_k(new)=b2_k(past) + \Delta b2_k \quad (8)$$

where δ_k functions to distribute errors from the output back to the previous layer, $(t_k-y_k)\ f'(y\_in_k)$ is the subtraction of the target with the production, δ_k is used to update weights between hidden layer and input layer, Δw_{jk} is weight correction, $\delta\alpha_k z_j$ is the learning rate (α), $\Delta b2_k$ is bias, w_{jk}(new) is the latest weight, $b2_k$(new) is the new bias, step 4 is performed for each hidden layer.

5. Each of hidden unit (z_j, j = 1,2,..p) sums up the input deltas (of the units in the upper layer):

$$\delta\_in_j = \sum_{k=1}^{m} \delta_k w_{jk} \quad (9)$$

Multiply this value by the derivative of the activation function to calculate the error information:

$$\delta_j = \delta\_in_j\ f'(z\_in_j) \quad (10)$$

Then calculate the weight correction:

$$\Delta v_{ij} = \alpha\ \delta_j\ x_i \quad (11)$$

And bias correction:

$$\Delta b1_j = \alpha\ \delta_j \quad (12)$$

$$v_{ij}(new) = v_{ij}(past) + \Delta v_{ij} \quad (13)$$

$$b1_j(new) = b1_j + \Delta b1_j \quad (14)$$

6. Test the stop conditions (check the correlation, RMSE, and epoch).

2.7. Prediction Evaluation

After completing the training and testing stages, the output results will be compared with the target. For each input, it is necessary to calculate the correlation coefficient (R) and error. The correlation coefficient (R) compares the predicted results and the actual value. If the calculation result of the R-value is closer to 1, then the prediction result will be close to the exact value or used as a target. The error function commonly used is the Root Mean Square Error (RMSE) which is the value of the prediction results error rate, and the smaller (closer to 0) the RMSE value, the more accurate the prediction results will be. The correlation coefficient formula (R) and RMSE are as follows [39].

$$r_{xy} = \frac{n(\sum XY) - (\sum X)(\sum Y)}{\sqrt{[n(\sum X^2) - (\sum X)^2]\,[n(\sum Y^2) - (\sum Y)^2]}} \quad (15)$$

where, r_{xy} = score correlation coefficient between variables, n = number of samples, X = first variable score, Y = the second correlated variable score.

$$RMSE = \sqrt{\frac{\sum_{i=1}^{n}(X_{obs,i} - X_{model,i})^2}{n}} \quad (16)$$

where, $X_{obs,i}$ = actual data value, $X_{model,i}$= prediction result value, N = the sum of the data, $\sum$ = the sum of the total value.

3. Results and Discussion

Training, testing, and validation have been carried out in each iteration to obtain the best ANN modelling results. The iteration process was carried out continuously until it produced the minimum RMSE value, the optimum value of training correlation, testing, and validation for each training function. The results of the ANN process are as shown in Table 1.

Table 1. The comparison of modelling results based on ANN parameters

Training Function	Parameter						Training		Testing		Validation	RMSE
	Lr	Epoch	Activation Function	Learning Function	Neuron	Layer	R^2	RMSE	R^2	RMSE		
CGB	0.1	350:1000	Purelin	LGD	10	1	0.906	0.242	0.960	0.235	0.927	0.342
CGB	0.1	410:1000	Purelin	LGD	20	1	0.919	0.506	0.922	0.459	0.901	0.451
CGB	0.1	431:1000	Purelin	LGD	30	1	0.921	0.841	0.927	0.742	0.864	0.482
CGB	0.01	450:1000	Purelin	LGDM	10,10	1&2	0.913	0.501	0.907	0.221	0.912	0.411
CGB	0.01	611:1000	Purelin	LGDM	10,20	1&2	0.914	0.503	0.940	0.511	0.905	0.511
CGB	0.01	425:1000	Purelin	LGDM	20,30	1&2	0.910	0.499	0.906	0.326	0.876	0.612
GD	0.1	528:1000	Purelin	LGD	10	1	0.503	0.892	0.582	0.921	0.445	0.627
GD	0.1	700:1000	Purelin	LGD	20	1	-0.837	0.999	-0.745	0.952	0.844	0.895
GD	0.1	650:1000	Purelin	LGD	30	1	0.391	0.921	0.414	0.742	0.473	0.774
GD	0.01	690:1000	Purelin	LGDM	10,10	1&2	0.904	0.220	0.963	0.609	0.902	0.524
GD	0.01	321:1000	Purelin	LGDM	10,20	1&2	0.909	0.621	0.975	0.600	0.890	0.433
GD	0.01	289:1000	Purelin	LGDM	20,30	1&2	0.907	0.613	0.947	0.612	0.918	0.412
GDX	0.1	2000:25000	Purelin	LGD	10	1	0.906	0.522	0.932	0.214	0.942	0.112
GDX	0.1	18828:25000	Purelin	LGD	20	1	0.914	0.241	0.920	0.331	0.931	0.364
GDX	0.1	3812:25000	Purelin	LGD	30	1	0.920	0.332	0.941	0.192	0.959	0.110
GDX	0.01	311:25000	Purelin	LGDM	10,10	1&2	0.899	0.420	0.943	0.219	0.960	0.213
GDX	0.01	1774:25000	Purelin	LGDM	10,20	1&2	0.895	0.115	0.985	0.072	0.994	0.022
GDX	0.01	287:25000	Purelin	LGDM	20,30	1&2	0.892	0.741	0.962	0.131	0.964	0.200

Based on Table 1, the results of the ANN process are shown in each iteration using several ANN parameters. The training function in this study consisted of the CGB, GD, and GDX trains. The learning parameters included learning rate (Lr) used at 0.1 and 0.01, maximum epoch 25000, purelin activation function, function Learning GD (LGD) and Learning GDM (LGDM), and the number of neurons in the hidden layer 10, 20, and 30. The number of hidden layers was divided into two; the first ANN process used one hidden layer and the second ANN process used two hidden layers.

From Table 1, it can be observed that the best ANN process was the GDX training function, purelin activation function, LGD, and LGDM learning functions, Lr 0.1 and 0.01, at the number of epochs 3812 from 25000 and 1774 from 25000, which produced the best correlation and lowest RMSE value. The results are described in the graphic plot in Figure 5.

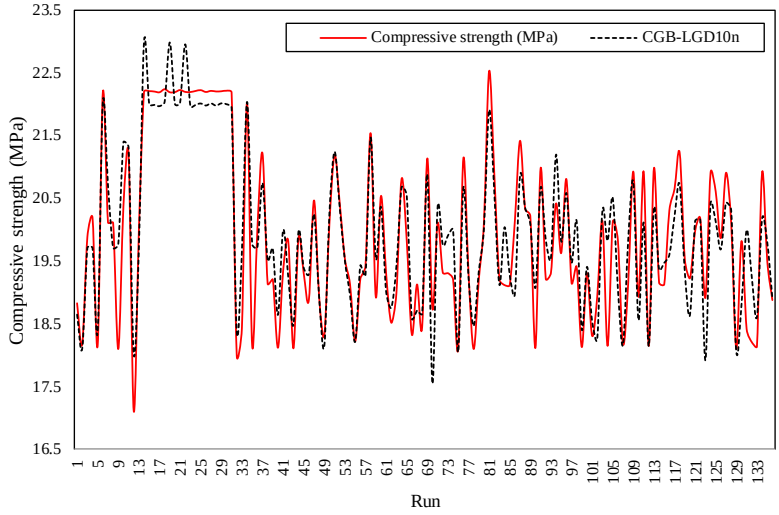

(a) T1: Learning rate 0.1, epoch 350 of 1000

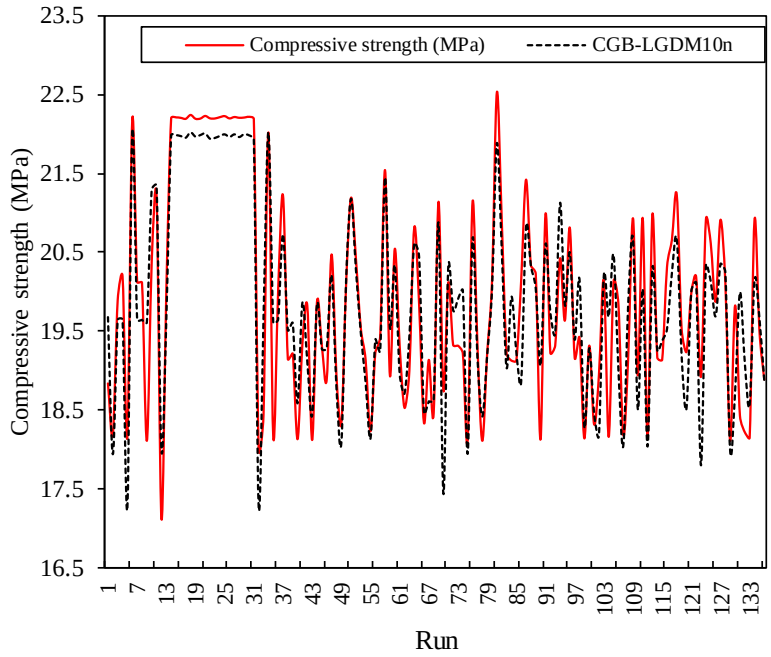

(b) T2: Learning rate 0.01, epoch

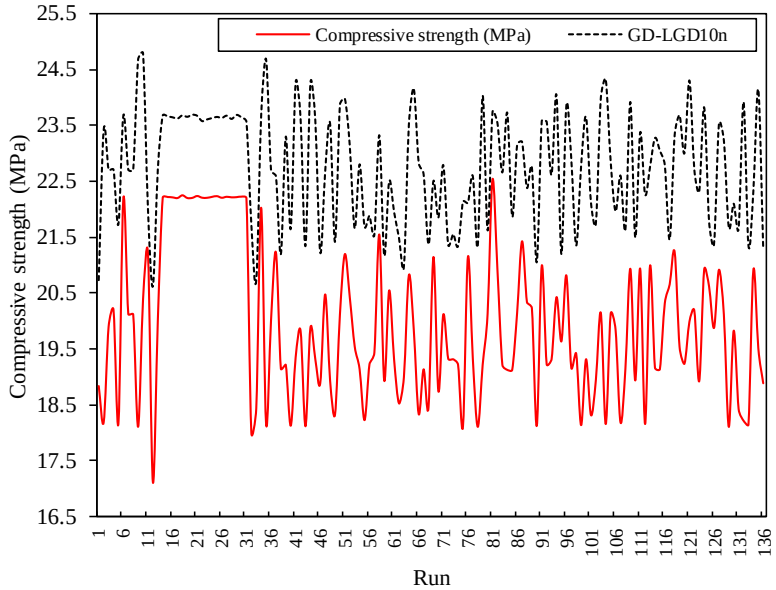

(c) T3: Learning rate 0.1, epoch 528 of 1000

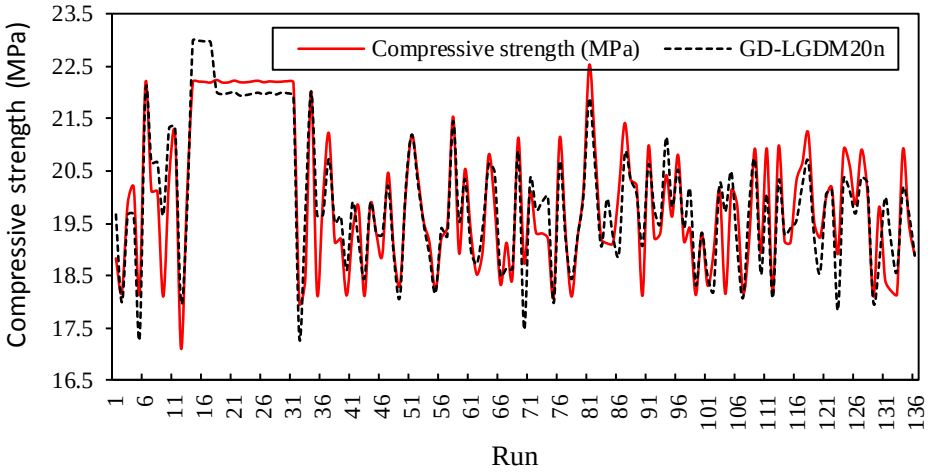

(d) T4: Learning rate 0.01, epoch 321 of 1000

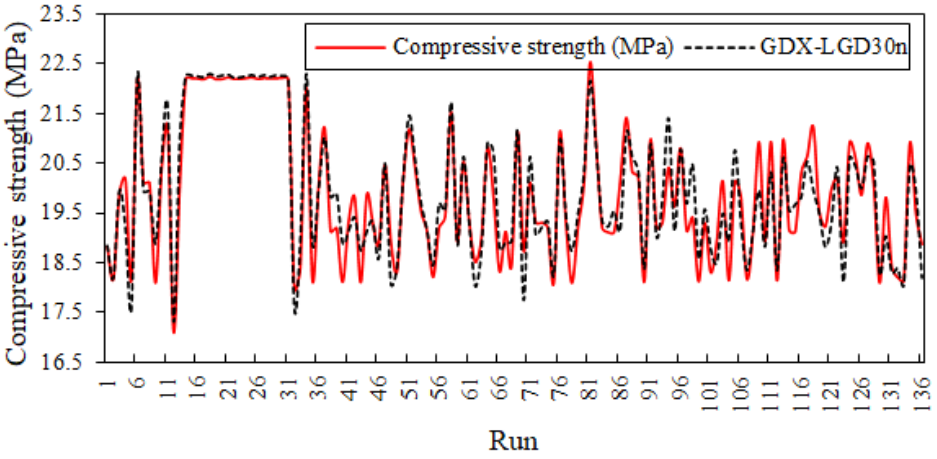

(e) T5: Learning rate 0.1, epoch 3812 of 25000

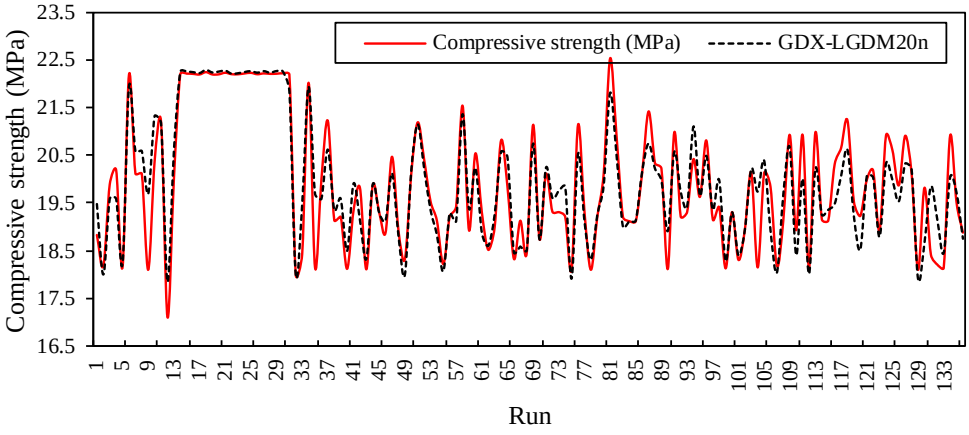

(f) T6: Learning rate 0.01, epoch 1774 of 25000

Figure 5. The comparison of actual vs. predicted value

Figure 5 shows a comparison plot of the actual data with the predicted results. The graph was chosen after checking all training functions and parameter combinations in the ANN process. From the six graphs above, it can be concluded that the learning rate of 0.1, epoch 3812 of 25000 and learning rate of 0.01, epoch 1774 of 25000 were the best prediction results and the lowest RMSE because the prediction results are close to the actual compressive strength (MPa) data. Figure 6. shows the average of the actual data and the predicted results with the training function and the combination of ANN parameters.

Figure 6 shows that the ANN models GXD-LGD30n and GDX-LGDM20n have excellent predictions and are close to the actual compressive strength (MPa) data. Figure 7 indicates the correlation values of the six training functions and the combination of ANN parameters.

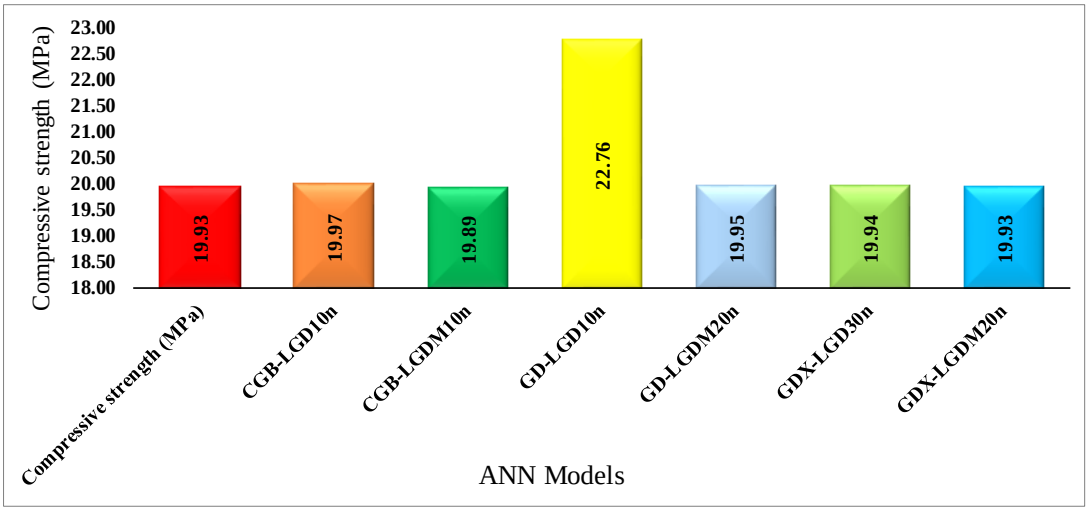

Figure 6. Overall average of actual data vs. predicted results

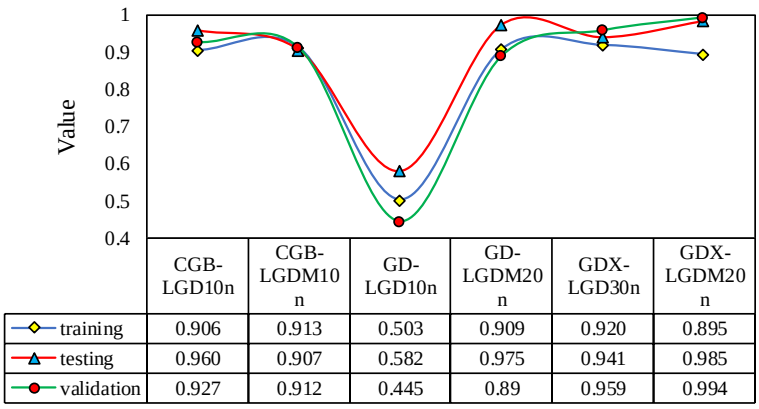

	CGB-LGD10n	CGB-LGDM10n	GD-LGD10n	GD-LGDM20n	GDX-LGD30n	GDX-LGDM20n
training	0.906	0.913	0.503	0.909	0.920	0.895
testing	0.960	0.907	0.582	0.975	0.941	0.985
validation	0.927	0.912	0.445	0.89	0.959	0.994

Figure 7. Actual vs Predicted Data Correlation

Figure 7 shows that the ANN model was inferior in the GD-LGD10n training function. In contrast, the GXD-LGD30n and GDX-LGDM20n ANN models at the training, testing, and validation stages have firm correlation values, and this is the recommended model for prediction. The R^2 values consistently exceed 0.9 at the training, testing, and validation stages, showing the model's high accuracy and robustness created using ANN. Specifically, the maximum R obtained in the testing sample is 0.941, while the minimum R^2 in the training sample is 0.920, with the validation R yielding even higher results than both. These results align with previous studies, where maximum and minimum R values exceeded 0.9 [31]. The RMSE value for each ANN model is shown in Figure 8.

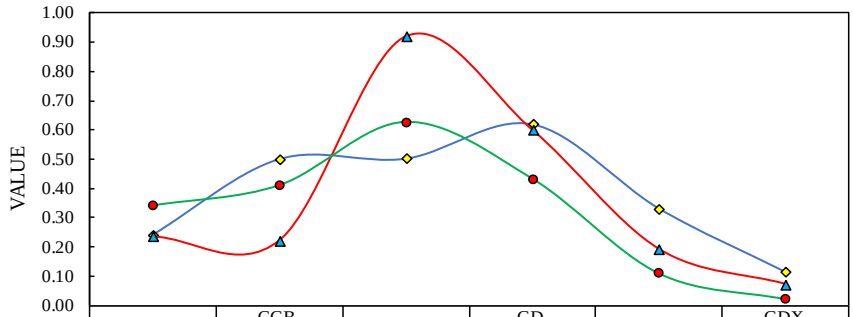

	CGB-LGD10n	CGB-LGDM10n	GD-LGD10n	GD-LGDM20n	GDX-LGD30n	GDX-LGDM20n
Training	0.242	0.501	0.503	0.621	0.332	0.115
Tetsing	0.235	0.221	0.921	0.600	0.192	0.072
Validation	0.342	0.411	0.627	0.433	0.110	0.022

Figure 8. The RMSE value for the ANN model

Figure 8 shows the RMSE value in each ANN model. The best ANN model is when it has the lowest RMSE value. From the six ANN models for comparison, the GXD-LGD30n and GDX-LGDM20n ANN training models obtained the

lowest RMSE values in each ANN training, testing, and validation when compared to other models, which were higher than the two models. Thus, the GXD-LGD30n and GDX-LGDM20n ANN models are excellent at predicting compressive strength (MPa). The error calculation results showed that it the ANN model exhibits the lowest RMSE, thus displaying the highest prediction accuracy according to the statistical performance conducted. This outcome is consistent with the results reported in a previous study [32].

Figure 9 shows the result of the GDX-LGD30n and GDX-LGDM20n ANN model processing with MATLAB at each training, testing, and validation epoch. The training and validation processes of the two models have a linear relationship and are strengthened by the prediction results in Figure 9.

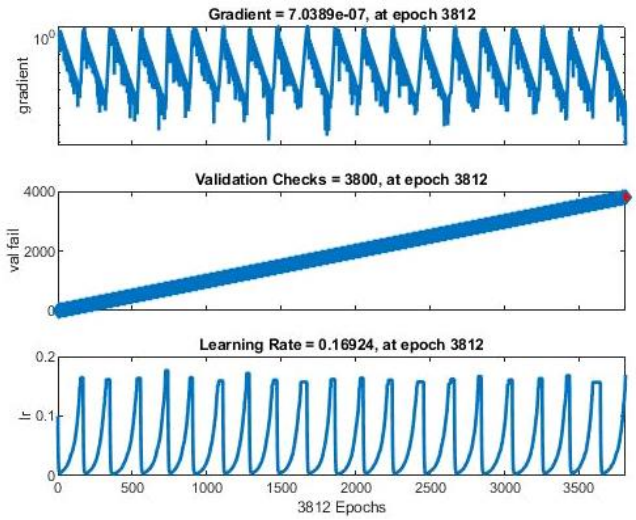

Training Process of GDX-LGD30n

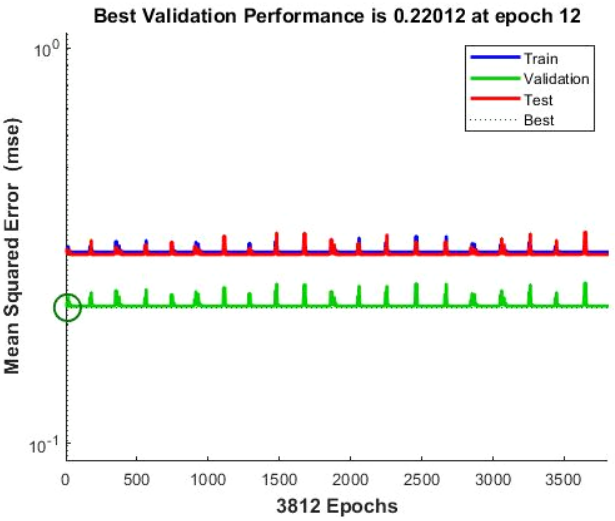

Best Validation GDX-LGD30n

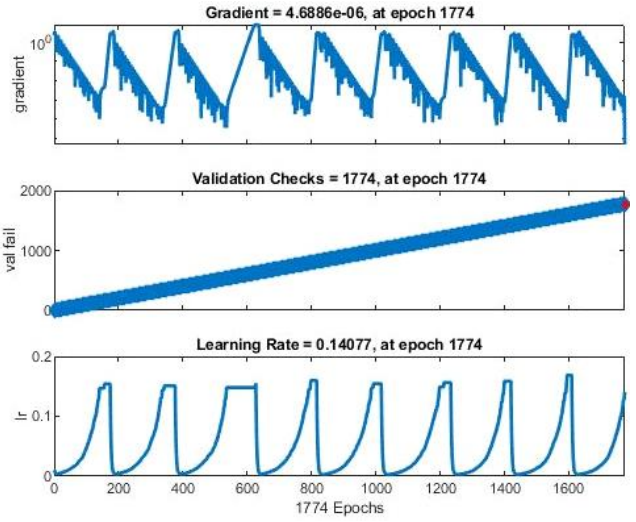

Training Process of GDX-LGDM20n

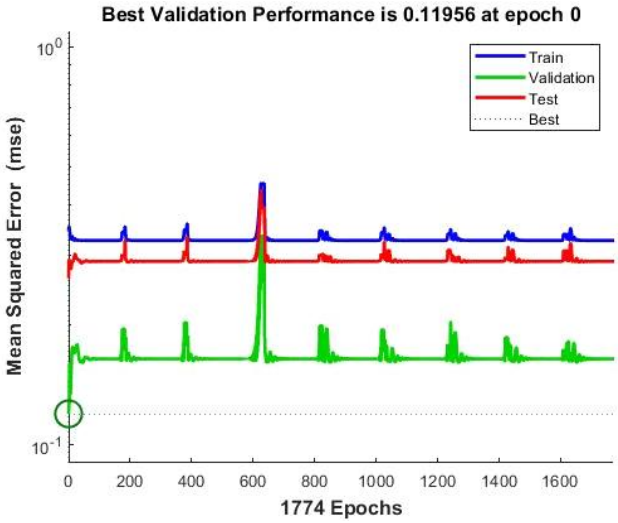

Best validation GDX-LGDM20n

Figure 9. ANN Model Validation and Training Status

The research findings obtained with the ANN model in this study are corroborated by previous studies, indicating that ANN demonstrates the predictive equation's adaptability to all types of modified geopolymer concrete mixtures in the future, thereby offering enhanced accuracy. The ANN model accurately predicts absorption rate as a function of binder content, basal fiber content, compressive strength, and changes in concrete mass [40]. Furthermore, other studies reveal that fly ash-based geopolymers utilizing a developed Neural Network model algorithm are potent tools for predicting geopolymer compressive strength [41]. Machine learning techniques applied to predict concrete compressive strength based on cellulose nanofibers yield R^2 >0.72, MAPE ≤ 0.1, and MAE ≤ 5, aligning with the standard of R^2 values exceeding 0.60 [42]. Despite proving superior performance, ANN necessitates substantial experience and computational resources [43]. The results of this study indicate that geopolymers utilizing nanosilica and CNCs, modeled using ANN methodology, exhibit the influence of nanosilica and CNCs on geopolymer compressive strength when applied at concentrations of 2%-4% and 1%-3%, respectively. The optimal ANN configuration entails utilizing the GDX training function, purelin activation function, LGD and LGDM learning

functions, with learning rates of 0.1 and 0.01, reaching 3812 epochs out of 25000 and 1774 epochs out of 25000, yielding the highest correlation values of 0.994 and 0.959, and the lowest RMSE values of 0.022 and 0.110. The results of the ANN model constructed based on actual data demonstrate its potential and utility for accurately simulating and predicting geopolymer cement compressive strength.

4. Conclusion

This study has successfully predicted the mixture of nanosilica and CNCs on the compressive strength of geopolymer cement with an ANN model. 70% data division for training, 15% for validation, 15% for testing the model, and a maximum of 25000 epochs used by combining ANN training function parameters obtained that, in general, the GDX training function produces optimal prediction results. Nanosilica is given with a concentration of 2%–4% and CNCs 1%–3% compressive strength prediction results obtained that the best ANN process is GDX training function, purelin activation function, LGD and LGDM learning functions, Lr 0.1 and 0.01 at the number of epochs 3812 of 25000 and 1774 of 25000 produces the best correlation coefficient of 0.994 and 0.959, the lowest RMSE values are 0.022 and 0.110. The ANN model developed based on actual data proved that the model has potential and is practical for accurate simulation to predict the compressive strength of geopolymer cement. The optimum compressive strength of 22.20 MPa was obtained by adding nanosilica and CNCs concentrations of 3.98 and 1%, respectively. There is an interaction between nanosilica and CNCs on the compressive strength of geopolymer cement. The addition of nanosilica has facilitated the formation of additional calcium silicate hydrate (C-S-H) gel, which is responsible for enhancing the compressive strength and durability of concrete. At the same time, CNCs have acted as nano-reinforcements within the geopolymer matrix, improving its tensile strength and crack resistance. Additionally, they might have contributed to the densification of the microstructure, resulting in enhanced compressive strength.

5. Declarations

5.1. Author Contributions

Conceptualization, C.R. and S.A.; methodology, S. and E.; validation, S.A. and S.; formal analysis, E. and J.A.; data curation, I. and M.M; writing—original draft preparation, C.R. and I.; writing—review and editing, M.M. and J.A. All authors have read and agreed to the published version of the manuscript.

5.2. Data Availability Statement

The data presented in this study are available in the article.

5.3. Funding

This research was funded by The Ministry of Education, Culture, Research, and Technology, Indonesia for a fundamental research scheme in 2023 with contract No. 189/E5/PG.02.00.PL/2023.

5.4. Conflicts of Interest

The authors declare no conflict of interest.

6. References

[1] Handayani, L., Aprilia, S., Abdullah, Rahmawati, C., Bakri, A. M. M. Al, Aziz, I. H., & Azimi, E. A. (2021). Synthesis of Sodium Silicate from Rice Husk Ash as an Activator to Produce Epoxy-Geopolymer Cement. Journal of Physics: Conference Series, 1845(1), 1–8,. doi:10.1088/1742-6596/1845/1/012072.

[2] Ahmad, J., Zhou, Z., & Martínez-García, R. (2022). A study on the microstructure and durability performance of rubberized concrete with waste glass as binding material. Journal of Building Engineering, 49(January), 104054. doi:10.1016/j.jobe.2022.104054.

[3] Wongsa, A., Kunthawatwong, R., Naenudon, S., Sata, V., & Chindaprasirt, P. (2020). Natural fiber reinforced high calcium fly ash geopolymer mortar. Construction and Building Materials, 241. doi:10.1016/j.conbuildmat.2020.118143.

[4] Rahmawati, C., Handayani, L., Muhtadin, Faisal, M., Zardi, M., Sapuan, S. M., Hadi, A. E., Ahmad, J., & Isleem, H. F. (2023). Optimization of Mortar Compressive Strength Prepared with Waste Glass Aggregate and Coir Fiber Addition Using Response Surface Methodology. Journal of Renewable Materials, 11(10), 3751–3767. doi:10.32604/jrm.2023.028987.

[5] Opiso, E. M., Tabelin, C. B., Maestre, C. V., Aseniero, J. P. J., Park, I., & Villacorte-Tabelin, M. (2021). Synthesis and characterization of coal fly ash and palm oil fuel ash modified artisanal and small-scale gold mine (ASGM) tailings based geopolymer using sugar mill lime sludge as Ca-based activator. Heliyon, 7(4), 6654. doi:10.1016/j.heliyon.2021.e06654.

[6] Naskar, S., & Chakraborty, A. K. (2016). Effect of nano materials in geopolymer concrete. Perspectives in Science, 8, 273–275. doi:10.1016/j.pisc.2016.04.049.

[7] Alvee, A. R., Malinda, R., Akbar, A. M., Ashar, R. D., Rahmawati, C., Alomayri, T., Raza, A., & Shaikh, F. U. A. (2022). Experimental study of the mechanical properties and microstructure of geopolymer paste containing nano-silica from agricultural waste and crystalline admixtures. Case Studies in Construction Materials, 16, 792. doi:10.1016/j.cscm.2021.e00792.

[8] Phoo-ngernkham, T., Chindaprasirt, P., Sata, V., Hanjitsuwan, S., & Hatanaka, S. (2014). The effect of adding nano-SiO2 and nano-Al2O3 on properties of high calcium fly ash geopolymer cured at ambient temperature. Materials and Design, 55, 58–65. doi:10.1016/j.matdes.2013.09.049.

[9] Assaedi, H., Shaikh, F. U. A., & Low, I. M. (2016). Influence of mixing methods of nano silica on the microstructural and mechanical properties of flax fabric reinforced geopolymer composites. Construction and Building Materials, 123, 541–552. doi:10.1016/j.conbuildmat.2016.07.049.

[10] Roopchund, R., Andrew, J., & Sithole, B. (2022). Using cellulose nanocrystals to improve the mechanical properties of fly ash-based geopolymer construction materials. Engineering Science and Technology, an International Journal, 25, 100989. doi:10.1016/j.jestch.2021.04.008.

[11] Rahmawati, C., Aprilia, S., Saidi, T., Aulia, T. B., Amin, A., Ahmad, J., & Isleem, H. F. (2022). Mechanical properties and fracture parameters of geopolymers based on cellulose nanocrystals from Typha sp. fibers. Case Studies in Construction Materials, 17, e01498. doi:10.1016/j.cscm.2022.e01498.

[12] Rahmawati, C., Aprilia, S., Saidi, T., Aulia, T. B., & Ahmad, I. (2022). Preparation and Characterization of Cellulose Nanocrystals from Typha sp. as a Reinforcing Agent. Journal of Natural Fibers, 19(13), 6182–6195. doi:10.1080/15440478.2021.1904486.

[13] Lazorenko, G., Kasprzhitskii, A., Mischinenko, V., & Kruglikov, A. (2022). Fabrication and characterization of metakaolin-based geopolymer composites reinforced with cellulose nanofibrils. Materials Letters, 308, 131146. doi:10.1016/j.matlet.2021.131146.

[14] Rocha Ferreira, S., Ukrainczyk, N., Defáveri do Carmo e Silva, K., Eduardo Silva, L., & Koenders, E. (2021). Effect of microcrystalline cellulose on geopolymer and Portland cement pastes mechanical performance. Construction and Building Materials, 288, 123053. doi:10.1016/j.conbuildmat.2021.123053.

[15] Ma, W., Qin, Y., Li, Y., Chai, J., Zhang, X., Ma, Y., & Liu, H. (2020). Mechanical properties and engineering application of cellulose fiber-reinforced concrete. Materials Today Communications, 22, 100818. doi:10.1016/j.mtcomm.2019.100818.

[16] Balea, A., Fuente, E., Blanco, A., & Negro, C. (2019). Nanocelluloses: Natural-based materials for fiber- reinforced cement composites. A critical review. Polymers, 11(3). doi:10.3390/polym11030518.

[17] da Gloria, M. Y. R., & Toledo Filho, R. D. (2021). Innovative sandwich panels made of wood bio-concrete and sisal fiber reinforced cement composites. Construction and Building Materials, 272, 121636. doi:10.1016/j.conbuildmat.2020.121636.

[18] Xie, X., Zhou, Z., Jiang, M., Xu, X., Wang, Z., & Hui, D. (2015). Cellulosic fibers from rice straw and bamboo used as reinforcement of cement-based composites for remarkably improving mechanical properties. Composites Part B: Engineering, 78, 153–161. doi:10.1016/j.compositesb.2015.03.086.

[19] Fu, T., Moon, R. J., Zavattieri, P., Youngblood, J., & Weiss, W. J. (2017). Cellulose nanomaterials as additives for cementitious materials. Cellulose-Reinforced Nanofibre Composites, Woodhead Publishing, Sawston, United Kingdom. doi:10.1016/b978-0-08-100957-4.00020-6.

[20] Fiore, V., Scalici, T., & Valenza, A. (2014). Characterization of a new natural fiber from Arundo Donax L. as potential reinforcement of polymer composites. Carbohydrate Polymers, 106(1), 77–83. doi:10.1016/j.carbpol.2014.02.016.

[21] Alvee, A. R., Malinda, R., Akbar, A. M., Ashar, R. D., Rahmawati, C., Mulyaningsih, S., & Putri, L. D. (2023). Influence of nanosilica and crystalline admixture on the short-term behaviour of buried underground geopolymer paste. AIP Conference Proceedings. doi:10.1063/5.0109331.

[22] Rahmawati, C., Aprilia, S., Saidi, T., Aulia, T. B., & Hadi, A. E. (2021). The effects of nanosilica on mechanical properties and fracture toughness of geopolymer cement. Polymers, 13(13), 2178. doi:10.3390/polym13132178.

[23] Hou, P., Kawashima, S., Kong, D., Corr, D. J., Qian, J., & Shah, S. P. (2013). Modification effects of colloidal nanoSiO2 on cement hydration and its gel property. Composites Part B: Engineering, 45(1), 440–448. doi:10.1016/j.compositesb.2012.05.056.

[24] Singh, L. P., Bhattacharyya, S. K., & Ahalawat, S. (2012). Preparation of size controlled silica nano particles and its functional role in cementitious system. Journal of Advanced Concrete Technology, 10(11), 345–352. doi:10.3151/jact.10.345.

[25] Jalal, M., Mansouri, E., Sharifipour, M., & Pouladkhan, A. R. (2012). Mechanical, rheological, durability and microstructural properties of high performance self-compacting concrete containing SiO_2 micro and nanoparticles. Materials and Design, 34, 389–400. doi:10.1016/j.matdes.2011.08.037.

[26] Korniejenko, K., Frączek, E., Pytlak, E., & Adamski, M. (2016). Mechanical Properties of Geopolymer Composites Reinforced with Natural Fibers. Procedia Engineering, 151, 388–393. doi:10.1016/j.proeng.2016.07.395.

[27] Correia, E. A., Torres, S. M., Alexandre, M. E. O., Gomes, K. C., Barbosa, N. P., & Barros, S. D. E. (2013). Mechanical performance of natural fibers reinforced geopolymer composites. Materials Science Forum, 758, 139–145. doi:10.4028/www.scientific.net/MSF.758.139.

[28] Chen, R., Ahmari, S., & Zhang, L. (2014). Utilization of sweet sorghum fiber to reinforce fly ash-based geopolymer. Journal of Materials Science, 49(6), 2548–2558. doi:10.1007/s10853-013-7950-0.

[29] Khademi, F., Jamal, S. M., Deshpande, N., & Londhe, S. (2016). Predicting strength of recycled aggregate concrete using Artificial Neural Network, Adaptive Neuro-Fuzzy Inference System and Multiple Linear Regression. International Journal of Sustainable Built Environment, 5(2), 355–369. doi:10.1016/j.ijsbe.2016.09.003.

[30] Behfarnia, K., & Khademi, F. (2017). A comprehensive study on the concrete compressive strength estimation using artificial neural network and adaptive neuro-fuzzy inference system. Iran University of Science & Technology, 7(1), 71-80.

[31] Bagheri, A., Nazari, A., & Sanjayan, J. (2019). The use of machine learning in boron-based geopolymers: Function approximation of compressive strength by ANN and GP. Measurement: Journal of the International Measurement Confederation, 141, 241–249. doi:10.1016/j.measurement.2019.03.001.

[32] McElroy, P. D., Bibang, H., Emadi, H., Kocoglu, Y., Hussain, A., & Watson, M. C. (2021). Artificial neural network (ANN) approach to predict unconfined compressive strength (UCS) of oil and gas well cement reinforced with nanoparticles. Journal of Natural Gas Science and Engineering, 88, 103816. doi:10.1016/j.jngse.2021.103816.

[33] Atoyebi, O. D., Awolusi, T. F., & Davies, I. E. E. (2018). Artificial neural network evaluation of cement-bonded particle board produced from red iron wood (Lophira alata) sawdust and palm kernel shell residues. Case Studies in Construction Materials, 9, 185. doi:10.1016/j.cscm.2018.e00185.

[34] Rahman, S. K., & Al-Ameri, R. (2023). Structural assessment of Basalt FRP reinforced self-compacting geopolymer concrete using artificial neural network (ANN) modelling. Construction and Building Materials, 397, 132464. doi:10.1016/j.conbuildmat.2023.132464.

[35] Verma, N. K., Meesala, C. R., & Kumar, S. (2023). Developing an ANN prediction model for compressive strength of fly ash-based geopolymer concrete with experimental investigation. Neural Computing and Applications, 35(14), 10329–10345. doi:10.1007/s00521-023-08237-1.

[36] Maheepala, M. M. A. L. N., Nasvi, M. C. M., Robert, D. J., Gunasekara, C., & Kurukulasuriya, L. C. (2023). Mix design development for geopolymer treated expansive subgrades using artificial neural network. Computers and Geotechnics, 161, 105534. doi:10.1016/j.compgeo.2023.105534.

[37] Nazar, S., Yang, J., Amin, M. N., Khan, K., Ashraf, M., Aslam, F., Javed, M. F., & Eldin, S. M. (2023). Machine learning interpretable-prediction models to evaluate the slump and strength of fly ash-based geopolymer. Journal of Materials Research and Technology, 24, 100–124. doi:10.1016/j.jmrt.2023.02.180.

[38] Igwe, K. C., Oyedum, O. D., Aibinu, A. M., Ajewole, M. O., & Moses, A. S. (2021). Application of artificial neural network modeling techniques to signal strength computation. Heliyon, 7(3), 6047. doi:10.1016/j.heliyon.2021.e06047.

[39] Awoyera, P. O., Kirgiz, M. S., Viloria, A., & Ovallos-Gazabon, D. (2020). Estimating strength properties of geopolymer self-compacting concrete using machine learning techniques. Journal of Materials Research and Technology, 9(4), 9016–9028. doi:10.1016/j.jmrt.2020.06.008.

[40] Rahman, S. K., & Al-Ameri, R. (2022). Experimental and Artificial Neural Network-Based Study on the Sorptivity Characteristics of Geopolymer Concrete with Recycled Cementitious Materials and Basalt Fibres. Recycling, 7(4), 1–19. doi:10.3390/recycling7040055.

[41] Khalaf, A. A., Kopecskó, K., & Merta, I. (2022). Prediction of the Compressive Strength of Fly Ash Geopolymer Concrete by an Optimised Neural Network Model. Polymers, 14(7). doi:10.3390/polym14071423.

[42] Anwar, A., Wenyi, Y., Jing, L., Yanwei, W., Sun, B., Ameen, M., Shah, I., Chunsheng, L., Mustafa, Z. U., & Muhammad, Y. (2023). Predicting the compressive strength of cellulose nanofibers reinforced concrete using regression machine learning models. Cogent Engineering, 10(1), 1–26,. doi:10.1080/23311916.2023.2225278.

[43] Yang, J., Fan, Y., Zhu, F., Ni, Z., Wan, X., Feng, C., & Yang, J. (2023). Machine learning prediction of 28-day compressive strength of CNT/cement composites with considering size effects. Composite Structures, 308, 116713. doi:10.1016/j.compstruct.2023.116713.